Scientific Journal of Impact Factor (SJIF): 4.72

e-ISSN : 2348-4470
p-ISSN : 2348-6406

International Journal of Advance Engineering and Research Development

National Conference On Nanomaterials, (NCN-2017)

Volume 4, Special Issue 6, Dec.-2017 (UGC Approved)

Structural, optical, antibacterial properties of cerium oxide nanoparticles prepared by green synthesis method using medicinal plant *Syzygiumcumini* leaf extract

S. Parvathy*, S. R. Elavarasu and R. Meena

Department of Chemistry, Government Arts College (Autonomous), Salem-7, TN, INDIA.

The cerium oxide nanoparticles (CeO_2 NPs) were prepared through the Syzygiumcumini leaf extracts. The X-ray diffraction studies confirmed that synthesized CeO_2 NPs were exhibited the cubic structure. The SEM image of CeO_2 NPs has exhibited spherical structure. From the EDAX spectral analysis, the elemental compositions were identified. The various functional groups were confirmed by FT-IR spectrum. The UV-Vis absorption spectra, the direct band gap was observed at 3.23eV for CeO_2 NPs. The antibacterial activity studies were done using K. pneumonia, S. aureus, S. dysenteriae and E. coli bacterial strain for CeO_2 NPs.

Introduction

Cerium oxide nanoparticles have been fascinating to effective technological applications, such as in solid-state electrolytes for electrochemical devices [1, 2], three way to using the catalysis in automobile consume systems [3, 4], abrasives for chemical–mechanical planarization [5], sunscreens for ultraviolet absorbents [6], the adsorption and reaction of formaldehyde [7], oxygen storage capacity [8], hybrid solar cells [9], H_2S removal [10] and luminescent materials for violet/blue fluorescence [11]. Recently year, the fabrication of nanoscale-size CeO_2 and investigation of the corresponding size-induced property changes, such as lattice expansion [12], phase transformation [13], and the blue-shift of absorption spectra [14]. Generally, CeO2 NPs were synthesized by physical and chemical methods such as hydrothermal, flame spray pyrolysis, sonochemical, microwave, sol–gel, and co-precipitation [15–21]. The green chemistry approaches to the development in phytosynthesis of metal and metal oxide NPs. This method offers a plenty of advantages such as cost-effectiveness, largescale commercial production and pharmaceutical applications.

S. cumini (L.) leaves are used in Indian folklore medicine coordination to possess numerous medicinal properties [22]. The leaves have been widely used to treat diabetes, constipation [23], leucorrhoea, stomachalgia, fever, gastropathy, strangury and dermopathy [22], and to inhibit blood discharges in the faeces [23]. The plant has acetyl oleanolic acid, triterpenoids, ellagic acid, isoquercitin, quercetin, kaempferol and myricetin in altered concentrations [24]. These compounds have been testified to possess antioxidant and free radical scavenging activities [25]. The chemical composition and antioxidant activity of *S. cumini* fruits have been studied recently [26,27].

In the present work, we synthesize CeO_2 NPs through an environmentally benign green pathway using *Syzygiumcumini*leaf extract and characterize the materials with suitable analytical tools. Further the efficiency of the materials studied as a function of antibacterial against some G+ and G- staining bacteria were carried out.

Materials and methods

Green synthesis CeO_2 NPs

The 10 g of finely divided green leaves of *Syzygiumcumini*was added to 100 mL of double distilled water and boiled at 60°C for 15 min. The solution was filtered through Whatmann No. 1 filter paper and the clear filtrate were collected and which was carry for further usage. Thereafter, add certain quantity of 0.1M solution of cerium nitrate to 100 mL of *Syzygiumcumini* leaf extract with constant stirring at 80 °C for 6h. Initially brown precipitate was formed and then it becomes a yellowish brown in color on continuous stirring. Further the precipitate was washed with water and followed by ethanol. The precipitate was annealed at 400 °C for 5h to get CeO_2. The Schematic diagram for the formation of CeO_2 NPs using *Syzygiumcumini* leaf extract is shown Fig. 1.

Antibacterial assay

The antibacterial activity of the CeO_2 NPs was carried out by the well diffusion method against the bacterial strains of (*K. pneumonia (1), S. aureus(2), S. dysenteriae(3), E. coli(4))* on Mueller hinton agar, according to the Clinical and Laboratory Standards Institute (CLSI). The media plate's Mueller hinton agar (MHA) was streaked with bacteria 2-3 times by rotating the plate at 60˚ angles for each streak to ensure the homogeneous distribution of the inoculums. After inoculation,

discs (6 mm Hi-Media) loaded with 1.5 mg/ml and 1.75 mg/ml, of the test samples were placed on the bacteria-seeded well plates using micropipettes. The plates were then incubated at 37 ˚C for 24 h. The inhibition zone around the well was measured and recorded. Amoxicillin (Hi-Media) was used as the positive controls against (*K. pneumonia (1), S. aureus(2), S. dysenteriae(3)* and *E. coli(4))* bacteria, respectively. The positive controls results were as compared to that of the efficacy of the test CeO_2 samples.

Characterization Techniques

The CeO_2 NPs were characterized by X-ray diffractometer (model: X'PERT PRO PANalytical). The diffraction patterns were recorded in the range of 20^o-80^o for the CeO_2NPs samples, where the monochromatic wavelength of 1.54 Å was used. The XPS measurements were performed with an XPS instrument (Carl Zeiss) equipment. The spectra were at a pressure using an ultra high vacuum with Al Kα excitation at 250 W. The samples were analyzed by Field Emission Scanning Electron Microscopy (Carl Zeiss Ultra 55 FESEM) with EDAX (model: Inca). The FT-IR spectra were recorded in the range of 400-4000 cm^{-1} by using a Perkin-Elmer spectrometer. The absorption spectra of CeO_2NPs were studied in the range between 200 and 800nm by Lambda 35 spectrometer.

X-ray diffraction patterns

The XRD patterns of green synthesizedCeO_2 NPs are shown in Fig. 2. The diffraction pattern corresponds to the cubic phase of CeO_2 [28]. The XRD peaks are located at angles (2θ) of 28.55, 33.90, 47.38 and 56.29 1 corresponding to (111), (200), (220), (311) and (222) planes of the CeO_2 NPs. The face-centered cubic phase of CeO_2 NPs exactly matches the JCPDS data card no: 34-0394. The synthesized CeO_2 NPs are more crystalline nature. The more crystalline nature of CeO_2 is due to the presence of many organic components involved in the NPs formation [29].

The lattice constant 'a' of CeO_2 can be calculated by using the relation,

$$\frac{1}{d^2} = \left(\frac{h^2 + k^2 + l^2}{a^2}\right)$$

The lattice constant 'a' is obtained through the relation a =$\sqrt{d^2(h^2 + k^2 + l^2)}$. The calculated 'a' value 5.414 Å for CeO_2 NPs. The unit cell volume can be calculated using the relation; V= a^3. The unit cell volume is found to be 158.69 $Å^3$ for CeO_2NPs.

The average crystallite size D of the sample is calculated after appropriate background corrections from X-ray line broadening of the diffraction peaks using Debye-Scherrer's formula.

$$\text{Average crystallite size D} = \frac{0.9\lambda}{\beta \cos\theta}$$

whereλ is the wavelength of X-ray used (1.5405 A), β is the angular peak width at half maximum in radians and θ is the Bragg's diffraction angle. The average crystallite size of D is 8.4 nm CeO_2 NPs.

Scanning Electron Microscope

The SEM analysis is one of the promising techniques for the morphological study of the sample and it gives important information regarding the shape and size of the particles. The surface morphology of the CeO_2 NPs synthesized by using *Syzgyiumcumini*leaf extract is shown in Fig. 3. The entire SEM image clearly shows the average size is nanoscale level for CeO_2 NPs. The synthesized CeO_2 NPs are exhibited spherical structure.

EDX analysis

In order to find out the elemental composition of the CeO_2NPs recording using EDAX spectra are shown in Fig. 4. Figure 4 shows clearly indicated that, only Ce and O were composed in the atomic percentage are found to be 33.93% and 66.07% for CeO_2 NPs.

FT-IR spectroscopic analysis

The FTIR spectra of CeO_2 NPs are shown in Fig. 5. In literature, the broad absorption in the frequency band 3750-3000 cm^{-1} are assigned to O-H stretching from residual alcohols, water and Ce-OH. From our result, the absorption band at 3402 $cm^{-1}$are attributed to the O-H mode for CeO_2 NPs respectively. The peaks at 2860 and 2950 cm^{-1} are due to symmetric and asymmetric stretching of C-H bonds [30]. However, symmetric and asymmetric C-H stretching observed at 2832 cm^{-1} and 2956 cm^{-1} for CeO_2 NPs. The absorption bands are caused by the vibration in CO_3^{2-} between 400 and 1800 cm^{-1} on the metallic cation groups. From the FT-IR result, small intensity absorption peak C=O observed at 1705 cm^{-1} for CeO_2 NPs. The band at 1654cm^{-1} corresponds to the bending of H-O-H, which is partly overlapping the O-C-O stretching band for CeO_2

sample. The C=O is stretching observed at 1518 and 1384 cm^{-1} for CeO_2 NPs. In the present work, the Ce-O stretching vibration is observed at 841, 723 and 545 cm^{-1} for CeO_2 NPs sample.

UV-Vis spectroscopy studies

The UV-Vis optical absorption spectra of CeO_2NPs are shown in Fig. 6. The absorption peak is found at 383 nm for CeO_2 NPs, and it's due to the photo excitation of electrons from the valence band to the conduction band.

The relation between the absorption coefficients α and the incident photon energy hυ can be written as

$$\alpha h\upsilon = A(h\upsilon - E_g)^n$$

Where E_g is the optical bandgap, A is the constant and the exponent n depends on the type of transition. Then = 1/2 for allowed direct transition, 2 for allowed indirect transition 3/2 and 3 for forbidden direct and indirect transitions respectively. The estimated direct band gap of the CeO_2 NPs is observed at 3.23 eV. It can be seen that the CeO_2 sample shows an increase in Eg by a value exceeding 0.04, compared to the bulk CeO_2 powders (Eg = 3.19 eV, determined by UV–Visible spectroscopy) [31].

Antibacterial activity

Antibacterial activity of CeO_2 NPs investigated the bacterial strains of (*K. pneumonia (1), S. aureus(2), S. dysenteriae(3) and E. coli(4))* are studied by well diffusion method as shown in Fig. 7. Figure 7clearly shows the area of zone inhibition of the antibacterial activity, which surrounds each CeO_2 NPs filled with test specimen.

The antibacterial efficacy of CeO_2 NPs is commonly influenced by ROS, which is mainly related to the size, larger surface area and increase in oxygen vacancies,.

From antibacterial activity CeO_2 NPs; CeO_2 NPs possessed similar antibacterial effect as compared to the other standard drug amoxicillin. The smaller sized NPs indeed have higher activity as antibacterial. The XRD pattern shows the particle size of CeO_2 NPs as 8.3 nm respectively. The smaller size can easily penetrate into bacterial membranes due to their large interfacial area, thus enhancing their antibacterial efficiency. The antibacterial efficiency of the CeO_2 NPs generally depends on the presence of ROS.

Conclusions

In summary, CeO_2 NPs prepared green synthesis method by using *Syzgyiumcumini* leaf extract. From the X-ray diffraction studies confirmed that the prepared nanoparticles were face-centered cubic phase. The average crystallite size was 8.4 nm for CeO_2 NPs. From the SEM images, CeO_2 NPs were exhibited spherical structure. Elemental compositions were identified by EDAX analysis. From FT-IR spectra, theCe-O stretching band observed at 545 cm^{-1} for CeO_2 respectively. The UV-Vis absorption spectra, the direct band gap was observed at 3.23 eV for CeO_2 NPs. The antibacterial activity studies were done using *K. pneumonia, S. aureus, S. dysenteriae and E. coli* bacterial strain treated with CeO_2 NPs.

References

1. M. Mogensen,N. M. Sammes, and G. A.Tompsett,*Solid State Ion.* 129, 63 (2000).
2. M. Yashima, S. Sasaki, Y. Yamaguchi,M. Kakihana, M. Yoshimura, and T. Mori, *Appl. Phys. Lett.* 72, 182 (1998).
3. K. Nikolaou,*Sci. Total Environ.* 235, 71 (1999).
4. M. Ozawa, *J. Alloys Compounds*, 275–277, 886 (1998)
5. X. D. Feng et al,*Science*, 312 1504 (2006).
6. N. Imanaka, T. Masui, H. Hirai, and G. Adachi,*Chem. Mater.* 15 2289 (2003).
7. J. Zhou and D. R. Mullins,*Surf. Sci.* 600 1540 (2006)
8. N. Kakuta, N. Morishima, N. Kotobuki,T. Iwase,T. Mizushima,Y. Sato and S.Matsuura *Appl. Surf. Sci.* 121/122 408 (1997).
9. M. Lira-Cantu and F. C. Krebs,*Sol. Energy Mater. Sol. Cells* 90 2076 (2006)
10. M.Flytzani-Stephanopoulos, M. Sakbodin and Z. Wang, Science 312 1508 (2006).
11. A. H. Morshed M. E.Moussa, S. M.Bedair, R. Leonard, S. X. Liu and N. El-Masry, Appl. Phys. Lett. 70 1647 (1997).
12. S. Tsunekawa, K. Ishikawa, Z-Q. Li, Y. Kawazoe, and A.Kasuya A, Phys. Rev. Lett. 85 3440 (2000).
13. Z. W. Wang, S. K.Saxena,V.Pischedda, H. P.Liermann and C. S.Zha, Phys. Rev. B 64 012102 (2001).
14. S.Tsunekawa,T. Fukuda and A.Kasuya, J. Appl. Phys., 87 1318 (2000).
15. F. Zhang,S. W. Chan, J. E.Spanier,E.Apak,Q. Jin,R. D. Robinson andI. P.Herman,Appl.Phys. Lett. 80 127–129(2002)

16. Campbell, C. T. &Peden, C. H. F. *Science.* 309, 713–714 (2005).
17. J. Hu, Y. Li, X. Zhou and M. Cai, Mater. Lett. 61 4989–4992 (2007).
18. H. Wang, J.J. Zhu, J.M. Zhu, X.H. Liao, S. Xu, T. Ding and H.Y. Chen, *Phys. Chem. Chem.Phys*. 4 3794–3799 (2002).
19. X.H. Liao, J.M. Zhu, J.J. Zhu, J.Z. Xu and H.Y. Chen, *Chem. Commun.* 937–938 (2001).
20. F. Czerwinski and J.A. Szpunar, J. Sol-Gel Sci. Technol. 9 103–114 (1997).
21. S.Y. Yao and Z.H. Xie, *J. Mater. Process. Technol.*186 54–59 (2007).
22. P. K. Warrier, V. P. K. Nambiar, C. Ramankutty, *Indian Medicinal Plants. Vol. 5, Orient Longman Ltd.: Hyderabad, India*,(1996).
23. M. J. Bhandary, K. R. Chandrashekar andK. M. Kaveriappa, J. Ethnopharmacol. 47, 149-158 (1995).
24. R. M. Rastogi, B. N.Mehrotra, *Central Drug Research Institute, Vol. 1,Lucknow, India*,(1990).
25. M. Tanaka, C. W. Kuei, Y. Nagashima, T.Taguchi, *Nippon Sui. Gakk.* 54, 1409-1414 (1998).
26. A. Banerjee, N. Dasgupta andB. De, *Food Chem.* 2005, 90, 727-733.
27. P. S. Benherlal andC. Arumughan, *J. Sci. Food Agric.* 87, 2560-2569 (2007).
28. L. S. RettyYadav, K. Manjunath, B. Archana, C.Madhu, H. Raja Naika, H.Nagabhushana, C.Kavitha, and G.Nagaraju, *Eur. Phys. J. Phys.* 131, 154-1 (2016).
29. S. Balasubramanian, D. Ganesh, and V. V. S. Surya Narayana, *Int. J. Pharm. Bio. Sci.*5, 258 (2014).
30. G. Munoz Hernandez, A. Escobedo Morales, and U. Pal, *Cryst.Growth Des*. 9, 297 (2009).
31. Z. Z. Orel and B. Orel, *Phys. Status Solidi B*186, K33 (1994)

Figure 1 A Schematic diagram for the formation of CeO_2 NPs by using *Syzygiumcumini* leaf extract

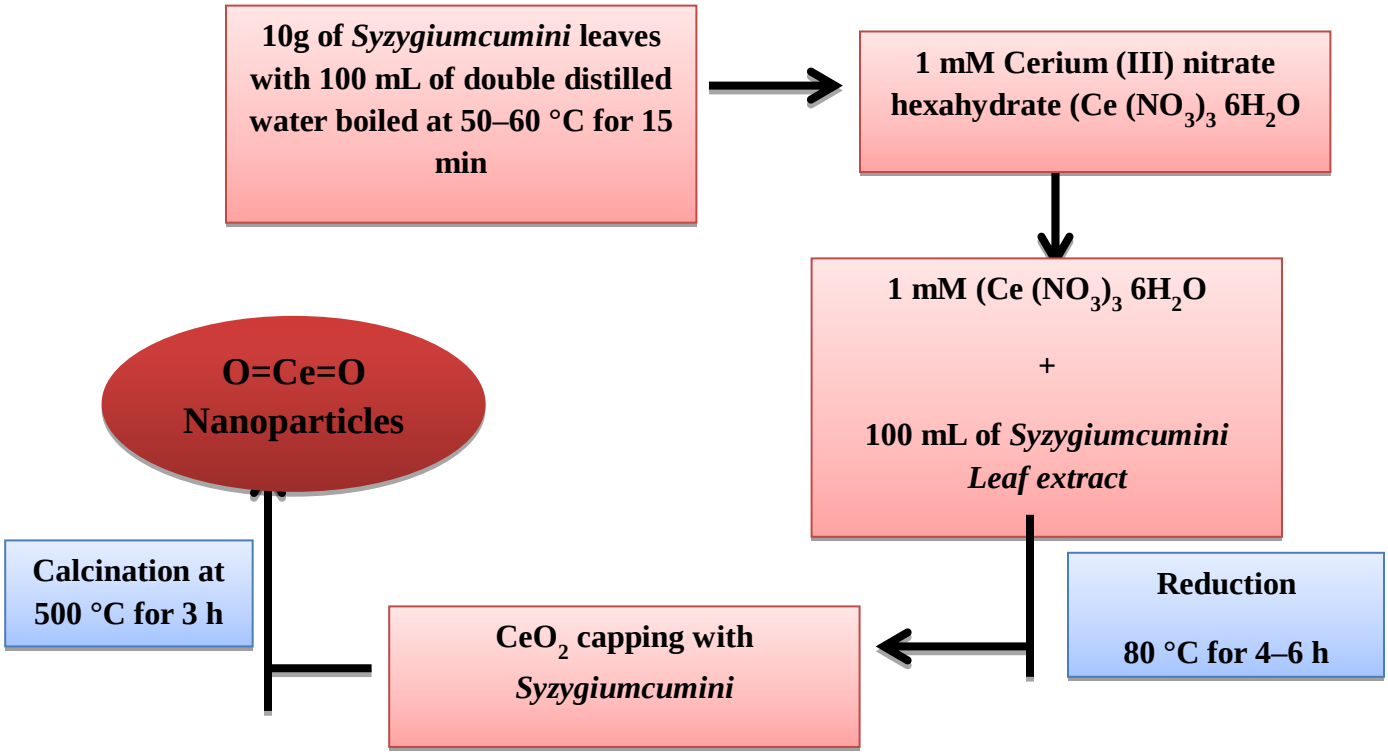

Figure 2 X-ray powder diffraction patterns of CeO_2 NPs by using Syzgyium*cumini leaf* extract.

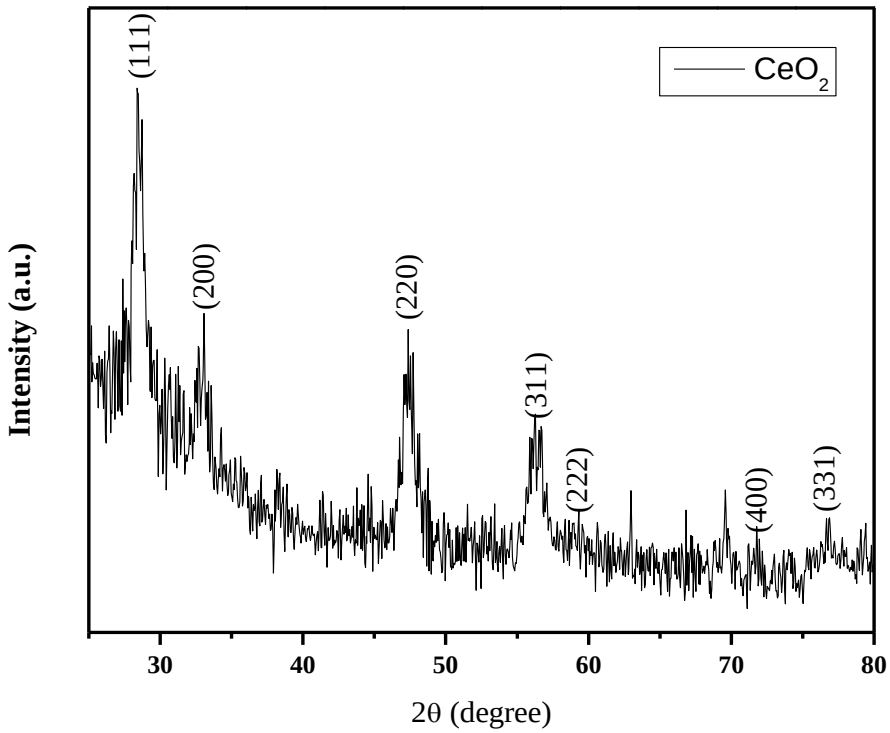

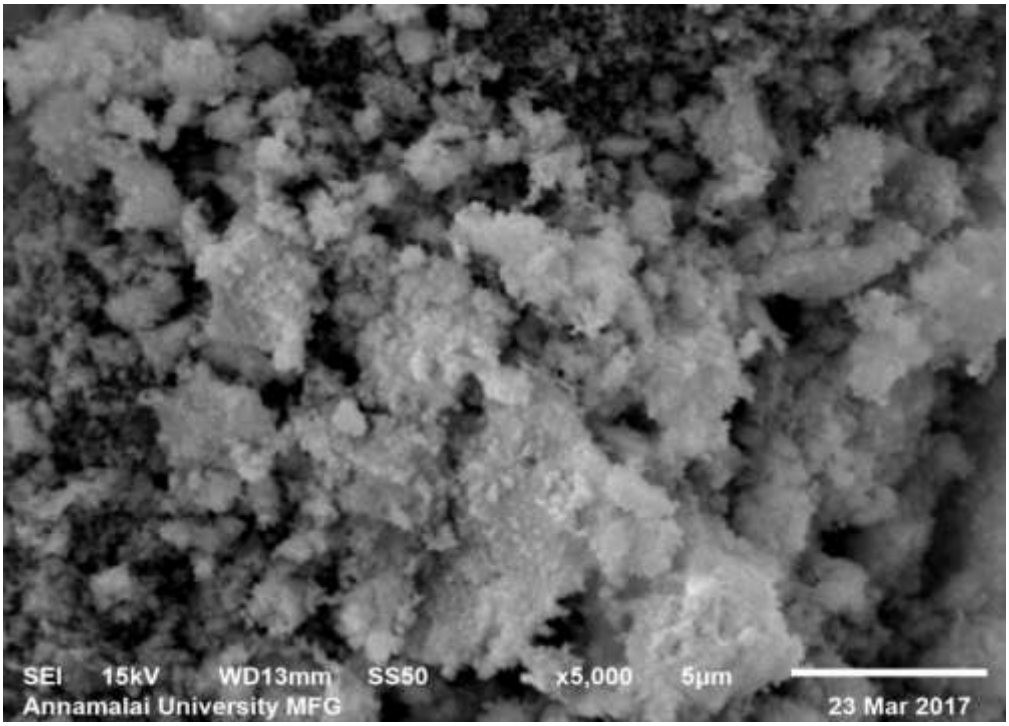

Figure 3 SEM images of CeO_2 NPs by using *Syzgyiumcumini leaf* extract.

Figure 4 EDAX Spectra of the CeO_2 NPs by using *Syzgyiumcuminii*leaf extract.

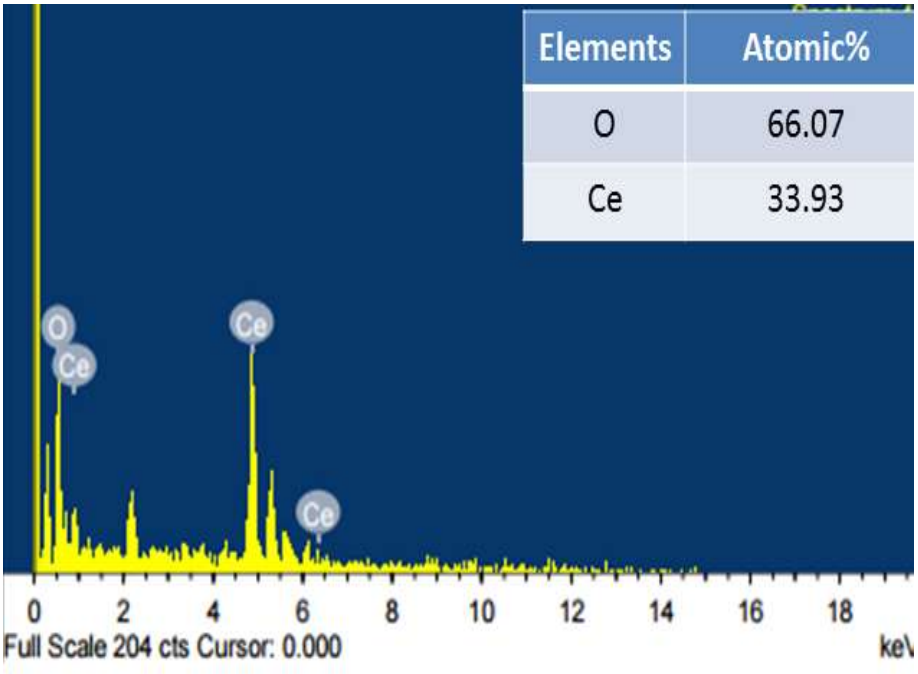

Figure 5 FTIR spectra of the CeO_2 NPs by using *Syzgyiumcuminii*leaf extract.

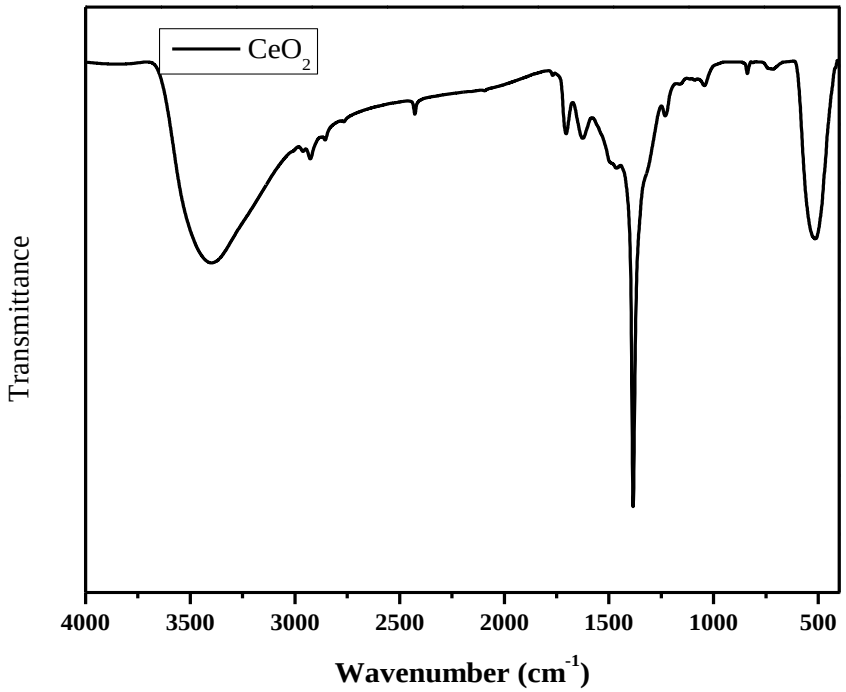

Figure 6 UV-Vis spectra of the CeO_2 NPs by using *Syzgyiumcuminii*leaf extract.

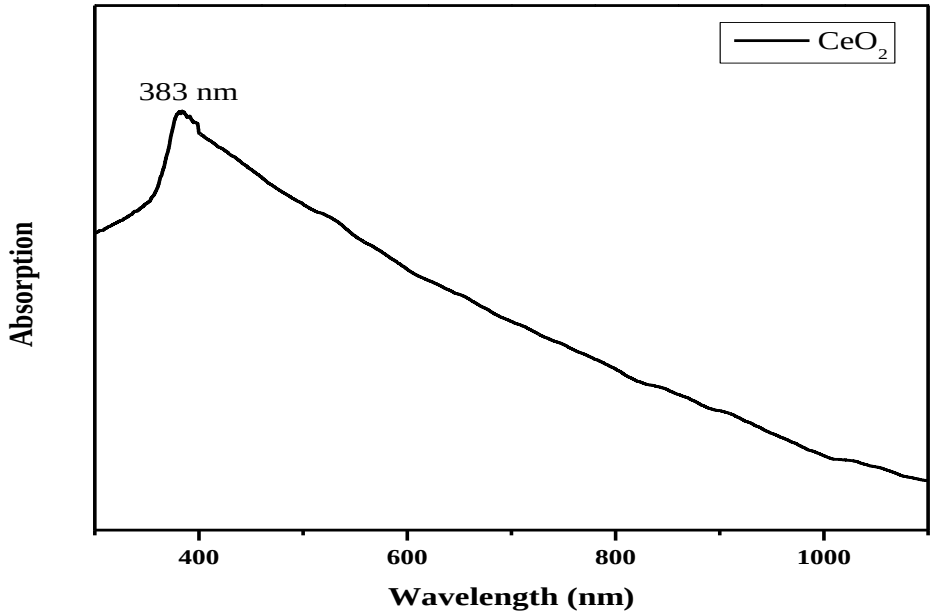

Figure 7 The antibacterial activity of the CeO_2 NPs tested against (*K. pneumonia* (1), *S. aureus* (2), *S. dysenteriae* (3) and *E. coli* (4))